## **Ceramics**



# Phase equilibria and metastability in the high-entropy $A_6B_2O_{17}$ oxide family with A = Zr, Hf and B = Nb, Ta

R. Jackson Spurling<sup>1,\*</sup> D, Chloe Skidmore<sup>1</sup>, Nathaniel S. McIlwaine<sup>1</sup>, and Jon-Paul Maria<sup>1,\*</sup>

Received: 12 February 2023 Accepted: 13 March 2023

© The Author(s), under exclusive licence to Springer Science+Business Media, LLC, part of Springer Nature 2023

#### **ABSTRACT**

The present work details experimental phase stabilization studies for the disordered, multi-cation  $A_6B_2O_{17}$  (A = Zr, Hf; B = Nb, Ta) system. We leverage both high-temperature in situ and ex situ X-ray diffraction to assess phase equilibrium and metastability in  $A_6B_2O_{17}$  ceramics produced via reactive sintering of stoichiometric as-received powders. We observe that the  $A_6B_2O_{17}$  phase can be stabilized for any stoichiometric combination of Group 4B and 5B transition metal cations (Zr, Nb, Hf, Ta), including ternary and quinary systems. The observed minimum stabilization temperatures for these phases are generally in agreement with prior calculations for each disordered A<sub>6</sub>B<sub>2</sub>O<sub>17</sub> ternary permutation, offering further support for the inferred cation-disordered structure and suggesting that chemical disorder in this system is thermodynamically preferable. We also note that the quinary (Zr<sub>3</sub>Hf<sub>3</sub>)(NbTa)O<sub>17</sub> phase exhibits enhanced solubility of refractory cations which is characteristic of other high-entropy oxides. Furthermore,  $A_6B_2O_{17}$  phases experience kinetic metastability, with the orthorhombic structure remaining stable following anneals at intermediate temperatures.

### Introduction

Rost et al. reported the first entropy-stabilized rock-salt oxide– $(Co_{0.2}Cu_{0.2}Mg_{0.2}Ni_{0.2}Zn_{0.2})O$ –in 2015. [1], In the subsequent years, multiple group identified additional single-phase, multi-constituent cation oxides to explore new properties and to test the entropic stabilization possibility [2–12]. Significant

interest persists to understand the thermodynamic and kinetic behavior of high-entropy systems and their relative roles in phase evolution [1, 13–16]. In such systems, the elemental diversity and configurational disorder generate an entropy-enthalpy exchange uncommon in naturally occurring materials that allows unusual cation coordinations with new property tunability across a variety of applications, ranging from dielectrics [17] to catalysis [18] to

Handling Editor: David Cann.

Address correspondence to E-mail: rjs7012@psu.edu; jpm133@psu.edu

https://doi.org/10.1007/s10853-023-08396-5

Published online: 03 April 2023



<sup>&</sup>lt;sup>1</sup>Department of Materials Science and Engineering, Pennsylvania State University, State College, USA

magnetism [19–21]. Recently, the  $A_6B_2O_{17}$  (A = Zr, Hf; B = Nb, Ta) oxide family was explored in this high configurational entropy context; specifically, work by McCormack and Kriven [22] and subsequently by Voskanyan et al. [23] provided a comprehensive structure solution and decomposition temperatures above which a series of these formulations are entropy-stabilized in the single-phase state [22, 23]. In the present report, we provide in situ and ex situ x-ray diffraction analysis to identify experimentally the temperature-time combinations that can produce  $A_6B_2O_{17}$  phases, to generate indications of their practical metastability and to provide companion data for existing predictions.

In 1973, Galy and Roth [24] first identified the orthorhombic structure of Zr<sub>6</sub>Nb<sub>2</sub>O<sub>17</sub> (space group Ima2). Recent work by McCormack and Kriven [22] demonstrates that  $A_6B_2O_{17}$  with A = Zr, Hf and B = Nb, Ta are isomorphous with the unit cell structure shown in Fig. 1. This layered structure features 6-, 7-, and 8-coordinated cation polyhedral (also modeled in Fig. 1). Subsequent work by Voskanyan et al. [23] predicted stabilization temperatures for each single-phase  $A_6B_2O_{17}$  isomorph. Notably, experiments show that fully disordered crystals form at lower temperatures than predicted for 50% ordered variants suggesting that cation sublattice disorder, and presumably configurational entropy, influences thermodynamic stability windows. Furthermore and Luo et al. [25] and Tan et al. [26] successfully produced multi-cation ( $\geq$  3)  $A_6B_2O_{17}$ , demonstrating an extension into more complex systems.

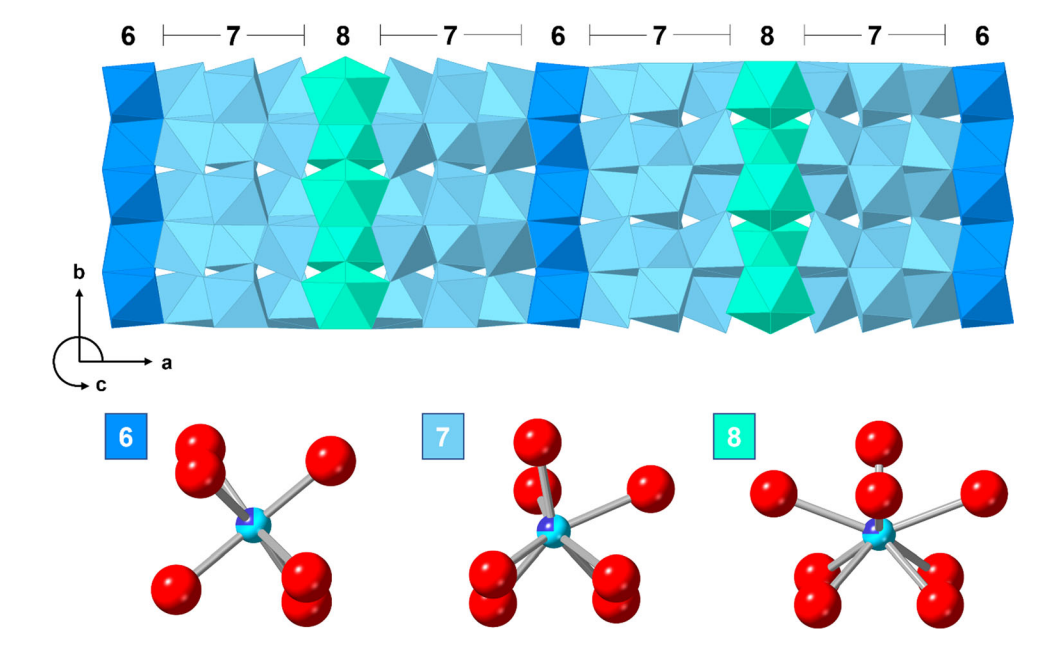
Current models for  $A_6B_2O_{17}$  (A = Zr, Hf; B = Nb, Ta) include cation disorder where A and B cations freely and randomly populate all polyhedral sites [22, 23]. Assuming complete cation disorder (and disregarding contributions from the anion sublattice with singular oxygen occupancy), the ideal configurational entropy is given by Eq. 1:

$$S_{\text{conf}} = -R \left[ x \left( \sum_{i=1}^{N} x_i ln x_i \right) + y \left( \sum_{i=1}^{N} y_i ln y_i \right) + z \left( \sum_{i=1}^{N} z_i ln z_i \right) \right]$$

$$\tag{1}$$

This configurational entropy expression is valid for a cation-disordered system with three different sites (in this case, 6-, 7-, and 8-coordinated positions, with the mole fraction of the ith cation on each site represented by  $x_i$ ,  $y_i$ , and  $z_i$ ). This yields a configurational entropy of 4.50R J/mol-K per unit cell for a ternary  $A_6B_2O_{17}$  phase, or, normalized per cation, 0.56R J/mol-K, where R is the universal gas constant [23]. In comparison  $(Co_{0.2}Cu_{0.2}Mg_{0.2}Ni_{0.2}Zn_{0.2})O$  features 1.61 J/mol-K entropy when fully disordered. As pointed out by McCormack and Kriven [22], disorder in the Zr<sub>6</sub>Ta<sub>2</sub>O<sub>17</sub> and Hf<sub>6</sub>Nb<sub>2</sub>O<sub>17</sub> isomorphs can be inferred directly from X-ray diffraction due to sufficient dissimilarity in atomic scattering factors of the constituent cations and consequently distinct diffraction patterns for fully ordered and fully

Figure 1 Model of the A6B2O17 structure and cation coordinations, per the structure solution provided by Galy and Roth [24] and McCormack and Kriven [22] (model rendered using CrystalMaker® software suite).





disordered crystals. Disorder in the  $\rm Zr_6Nb_2O_{17}$  and  $\rm Hf_6Ta_2O_{17}$  systems is generally inferred from their isomorphs because atomic scattering contrast between these cation pairs does not produce sufficient diffraction contrast. In the context of prior work, the present experiments monitor temperature thresholds for phase-evolution in these more challenging  $A_6B_2O_{17}$  systems and contribute to understanding phase stabilization in a composition spectrum.

We believe that  $A_6B_2O_{17}$  system crystals are special among many-cation solid solution formulations because it becomes entropy stabilized at high temperatures [23] despite its distribution of metal ions on three dissimilar lattice sites in a low-symmetry structure. This is different than other examples where a high-symmetry cubic host like rocksalt, spinel, or perovskite is more common. Furthermore, the orderdisorder transition shuffles cations with different preferred valence states among 6-, 7-, and 8-corrdinated oxygen polyhedral, which may produce interesting property modifications. As such, we feel a more granular exploration of the stabilization temperatures with a more rigorous comparison of structure evolution at high temperatures in the context of existing calculations [23] is warranted and endeavor to provide this analysis in the present manuscript.

#### **Methods**

 $A_6B_2O_{17}$  ceramics are prepared by conventional hightemperature, pressureless, solid-state reactive sintering. Stoichiometric amounts of as-received powder (ZrO<sub>2</sub>, TOSOH, 99.87%; Nb<sub>2</sub>O<sub>5</sub>, Sigma-Aldrich, 99.99%; HfO<sub>2</sub>, Sigma-Aldrich, 98%; Ta<sub>2</sub>O<sub>5</sub>, Sigma-Aldrich, 99.5%) are ball milled in methanol (Fisher Scientific, Grade: Certified ACS Reagent) using pristine yttrium-stabilized zirconia media for 30 h. X-ray diffraction scans of the as-received powders are provided in the Supplementary Materials. Powders are air-dried at 100 °C to drive off methanol for at least 2 h, followed by uniaxial pressing to form  $\sim 1$ g pellets in a 0.5 inch cylindrical steel die. Green bodies are air sintered at T = 1300 °Cfor 12 h to obtain phase-pure ceramics. A combination of scanning electron microscopy (Zeiss Sigma) and X-ray diffraction (Panalytical Empyrean, Bragg-Brentano geometry, Cu K $\alpha$  source,  $\lambda = 1.54$  Å) is used to identify the temperature and time combinations that produce the single-phase state. For high-temperature X-ray diffraction studies (Emyprean II Malvern Panalytical, Co K $\alpha$  source,  $\lambda$  = 1.79 Å, Anton-Paar HTK 1200N high-temperature stage; scans converted back to Cu K $\alpha$  2 $\theta$  positions), green bodies were subjected to single-ramp heat treatments with measurements collected every 10 °C from 600 to 1150 °C; a batch program with a 2 °C/min ramp rate and 2 min dwell at temperature prior to each measurement was used. Ex situ reaction studies at lower temperatures were conducted to study minimum temperatures for phase stability.

#### Results and discussion

X-ray diffraction data for conventionally fired samples indicate that all proposed permutations in the  $A_6B_2O_{17}$  (A = Zr, Hf; B = Nb, Ta) family, including the four ternary systems and one quinary system, adopt the orthorhombic  $A_6B_2O_{17}$  structure at sufficiently high temperature and time exposures. As an initial high-temperature thermodynamic stability test, a sample set (including the four ternaries and one quinary composition) were reacted at 1300 °C for 12 h. X-ray diffraction patterns for the entire set are shown in Fig. 2; a logarithmic intensity scale is used so that minor constituents are maximally visible. All compositions fully form orthorhombic  $A_6B_2O_{17}$  following this heat treatment, indicating thermodynamic stability at high temperature and practical metastability upon cooling. This observation is in agreement with both McCormack and Kriven [22] and Voskanyan et al. [23], who synthesized ternary  $A_6B_2O_{17}$  phases in a similar thermal budget regime. We note that cooling from high temperature was initially 10 °C/min and then slowed below approximately 600 °C to the natural cooling rate of the box furnace.

It is notable that, despite the existence of multiple isomorphous ternary and quaternary compounds, the quinary system remains stable and does not decompose into any of its end member derivatives. This apparent stability of the single-phase quinary structure is further supported by scanning electron microscopy and energy-dispersive spectroscopy, which indicate microstructural homogeneity and uniform cation dispersion, at least over micron length scales (Fig. 3). Based on the calculations by



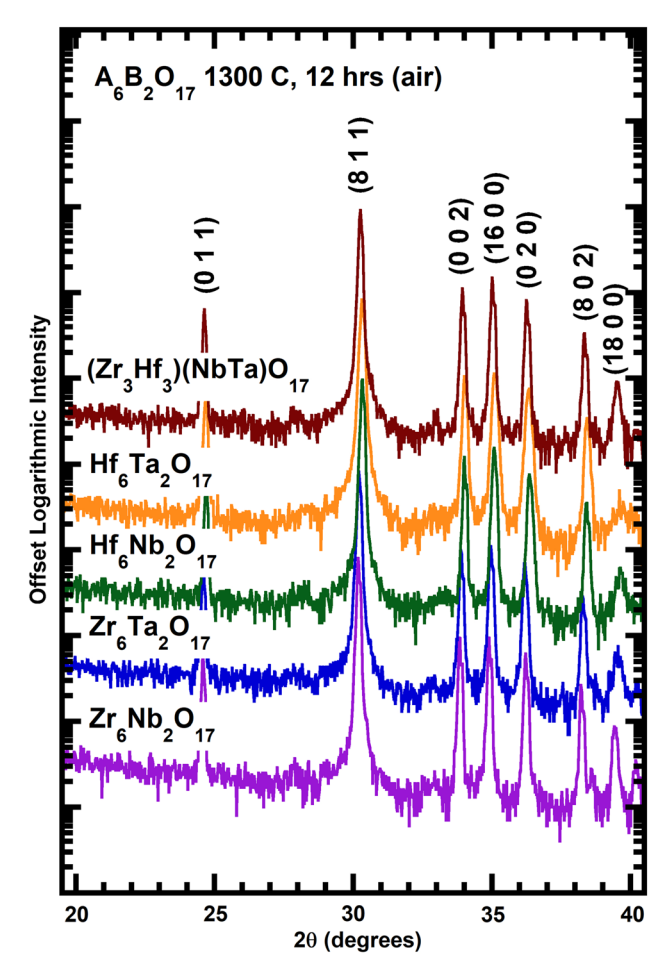


**Figure 2** X-ray diffraction patterns ( $\theta$ – $2\theta$  geometry) for all ceramic formulations heat treated to a maximum temperature of 1300 °C. Intensity is shown on a logarithmic scale with an offset for maximum visibility. In all cases, the  $A_6B_2O_{17}$  phase is predominant, indicating, at least, thermodynamic stability at elevated temperature. For the less refractory compositions the transformation is closer to completion.

Voskanyan et al. [23], the  $A_6B_2O_{17}$  family members should have substantially positive formation enthalpies. Consequently, the observed  $A_6B_2O_{17}$  oxide solid solution stability s likely results from configurational entropy contributions which are maximized in a fully disordered cation sublattice.

McCormack and Kriven [22] used X-ray diffraction to demonstrate disorder in Zr<sub>6</sub>Ta<sub>2</sub>O<sub>17</sub> and Hf<sub>6</sub>Nb<sub>2</sub>O<sub>17</sub> based on cation scattering factor differences that produce distinguishable reflections for the ordered versus disordered structures; moreover, calculations by Voskanyan et al. [23] predict minimum stabilization temperatures for ternary  $A_6B_2O_{17}$  phases that consider cation sublattice disorder. They calculate low-temperature thresholds at which each ternary  $A_6B_2O_{17}$  isomorph becomes stable (Table 1). To date, however, stabilization temperatures have not been isolated experimentally. Doing so is a particular challenge given the refractory nature of the constituent cation species as well as the slow diffusion and kinetic metastability which often accompany disordered many-cation oxides [6].

As an attempt to identify stability thresholds on heating, four ceramic formulations were analyzed using in situ high-temperature X-ray diffraction to monitor the reaction sequence of binary powder mixtures upon initial heat treatment. To establish a reference frame, the four ternary formulations were analyzed initially between room temperature and 1150 °C, the maximum temperature available to our instrumentation. Figure 4 shows intensity-temperature-two-theta maps between 600 °C and 1150 °C for the Zr–Nb, Zr–Ta, Hf–Nb, and Hf–Ta combinations. Reactions that form  $A_6B_2O_{17}$  begin at 910 °C, 1030 °C, 1000 °C, and 1150 °C, respectively. The individual

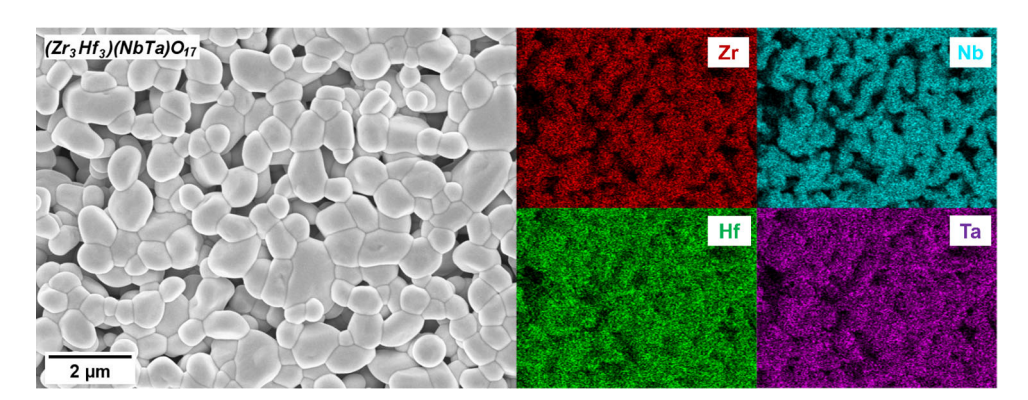


**Figure 3** Scanning electron micrograph and accompanying energy-dispersive spectroscopy maps for the quinary (Zr<sub>3</sub>Hf<sub>3</sub>)(NbTa)O<sub>17</sub> high-entropy isomorph. Elemental maps

indicate homogenous cation dispersion at the  $\mu m$  length-scale, with atomic fractions following the batch stoichiometry.



**Table 1** Formation enthalpies and minimum stabilization temperatures (i.e. decomposition following  $A_6B_2O_{17} \leftrightarrow 6AO_2 + 5B_2O_5$ ) for ternary  $A_6B_2O_{17}$  phases as calculated by Voskanyan et al. [23] using drop-melt calorimetry

Oxide	$\Delta H_f$ (kJ/mol)	$\Delta S_{conf}$ (J/mol K)	$T_{c,100\%}$ (K)	T <sub>c,50%</sub> (K)
Hf <sub>6</sub> Ta <sub>2</sub> O <sub>17</sub>	$42.94 \pm 7.03$	37.402	$1148 \pm 188$	$2296 \pm 376$
$\mathrm{Hf_6Nb_2O_{17}}$	$38.44 \pm 6.75$	37.402	$1028 \pm 180$	$2055 \pm 360$
$Zr_6Ta_2O_{17}$	$33.64 \pm 5.42$	37.402	$899 \pm 145$	$1798 \pm 290$
$Zr_6Nb_2O_{17}$	$35.52 \pm 6.45$	37.402	$950 \pm 172$	$1899 \pm 344$

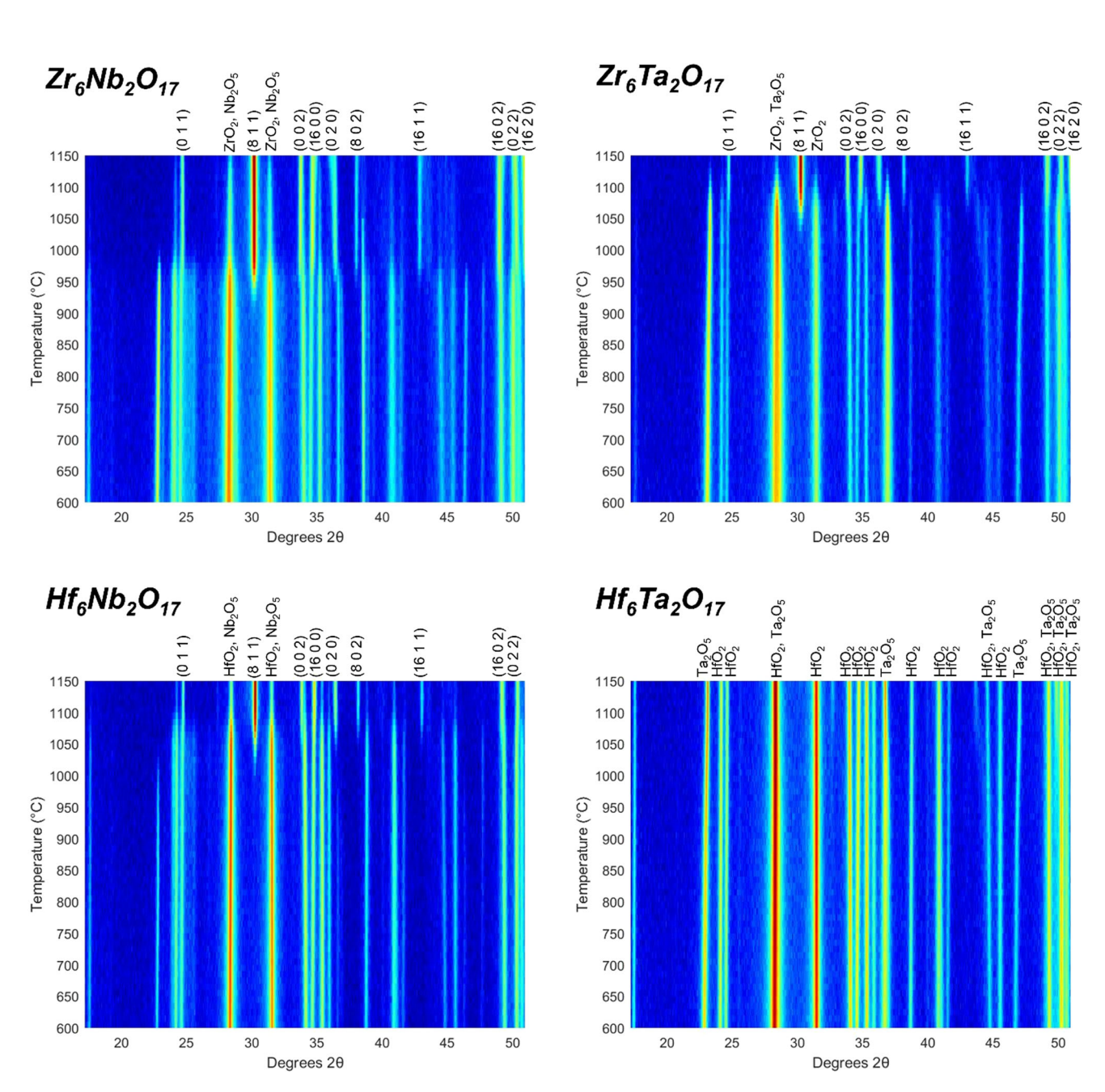


**Figure 4** High-temperature in situ X-ray diffraction plots are shown for each ternary  $A_6B_2O_{17}$  phase. Initial formation of the high-temperature phase is observed for all isomorphs following a

rough trend with increasingly refractory constituent cation combinations; a combination of thermodynamic stabilization and variable kinetic transport likely contribute to this trend.



reaction initiation temperatures are determined by examining line scans for where the  $A_6B_2O_{17}$  811 peak emerges. We note that while the intensity plots do not show prominent  $A_6B_2O_{17}$  formation for the Hf-Ta combination, close examination of the line scan at 1150 °C shows the emergence of a small peak, indicating that the reaction will proceed at this temperature. This modest temperature trend is generally aligned with the average melting points of the constituent oxides. It is important to note that these temperature trends may be associated with thermodynamic stability differences or may simply reflect differences in reaction kinetics; discriminating between these possibilities would require additional time-dependent studies. An additional challenge is posed in the frequent overlap in precursor X-ray peaks, which make it difficult to isolate the disappearance of individual precursor components. This is a result of the presence of similar phases in the binary oxides, as well as the chemically derived, polymorphic nature of some precursors. To assist in precursor identification, we provide powder diffraction scans in the Supplementary Materials (Fig. S1).

In addition to these in situ high-temperature X-ray diffraction experiments, a series of parallel experiments were conducted ex situ at lower temperatures with increased dwell times to observe potential phase formation isothermally on a time axis. In this experimental suite, samples of each ternary  $A_6B_2O_{17}$  were reacted at 850 °C, 950 °C, and 1000 °C, respectively, for 24 h, with subsequent characterization by X-ray diffraction. An additional run was conducted for Hf<sub>6</sub>Ta<sub>2</sub>O<sub>17</sub> at 1000 °C for 60 h. to observe clearer high-temperature phase formation. The resulting scans are displayed in Fig. 5 by composition for each temperature. We use the 811 peak appearance (the most prominent peak occurring at  $\sim 30^{\circ}2\theta$ ) as the indicator of initial phase formation. The 811 emerges in  $Zr_6Nb_2O_{17}$  after 850 °C and 24 h, in  $Zr_6Ta_2O_{17}$  and Hf<sub>6</sub>Nb<sub>2</sub>O<sub>17</sub> after 950 °C and 24 h, and in Hf<sub>6</sub>Ta<sub>2</sub>O<sub>17</sub> after 1000 °C and 60 h. Again, these transformation temperatures scale with the average refractoriness of the component binaries. Since these solid-state reactions involving multiple component powders are slow, they do not allow direct conclusions regarding thermodynamic stability temperature windows. It is possible (and perhaps likely) that the transition temperatures for each isomorph are in fact lower than those presently observed, and determining those

values may require timescales beyond a practical experimental scope.

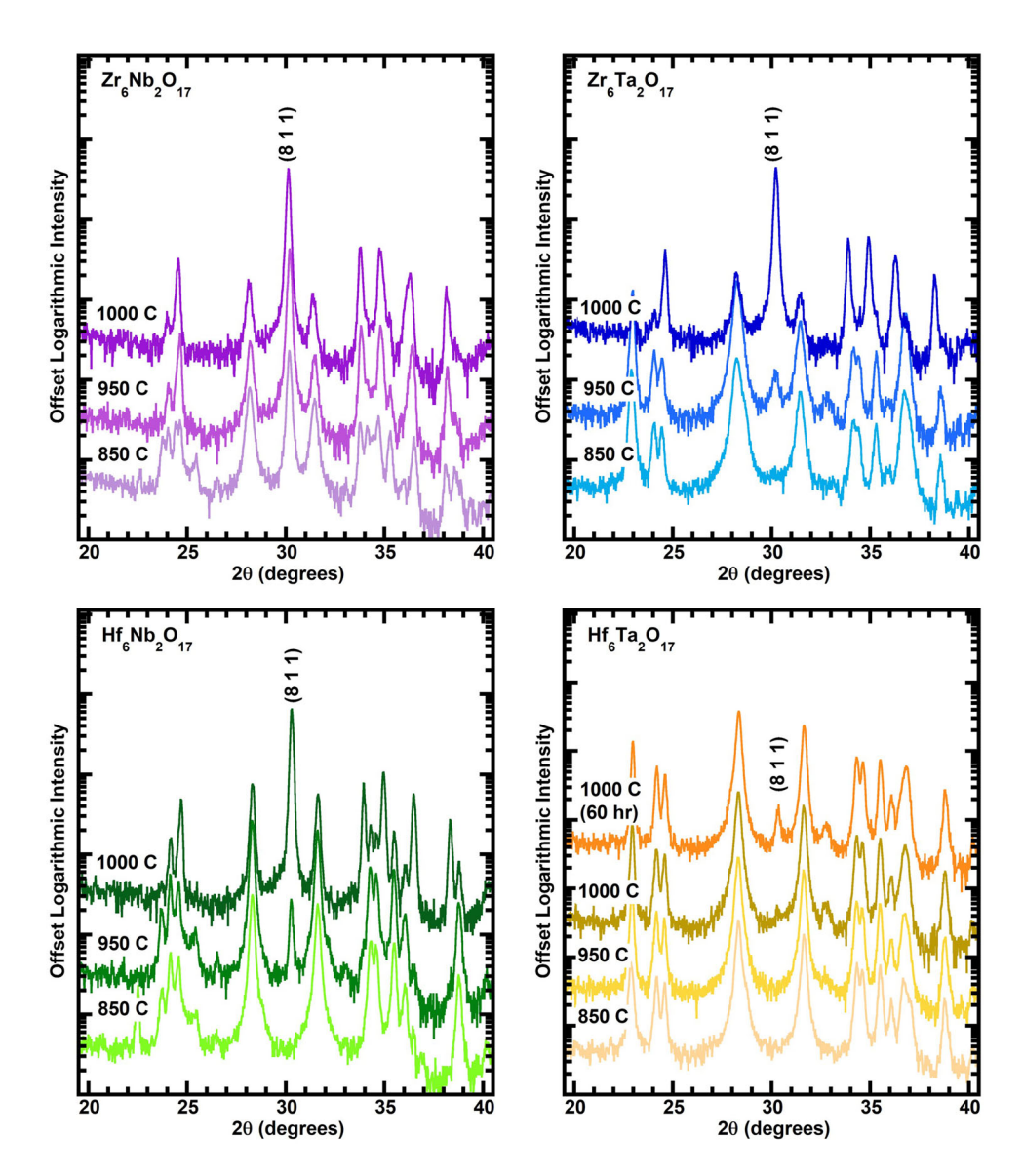
Nonetheless, these stabilization temperatures (which probably approach an upper limit) are in-line with the calculations by Voskanyan et al. [23] provided that these ceramics exist in the fully or highly cation-disordered state. We use the least refractorythus faster reacting-composition as an illustrative comparison. Zr<sub>6</sub>Nb<sub>2</sub>O<sub>17</sub> starts to form as low as 910 °C in our in situ experiment; however, our ex situ experiment shows significantly more  $A_6B_2O_{17}$  phase formation after 24 h at 850 °C, suggesting that phase formation is kinetically limited during the in situ diffraction experiment. Voskanyan et al. [23] predict a transformation window into the  $A_6B_2O_{17}$  disordered structure between 505 °C and 849 °C and the 50% disordered structure between 1282 °C and 1970 °C. The presently observed onset of  $A_6B_2O_{17}$ phase formation aligns well with the disordered system where all cations occupy the 6-, 7-, and 8-coordinated lattice positions randomly; moreover, per the previous discussion, it may be possible to observe phase formation at even lower temperatures at significantly longer timescales. Similar comparisons can be made or all other compositions suggesting that we presently observe the disordered structures.

In addition to the in situ and ex situ high-temperature X-ray diffraction experiments conducted on the ternary  $A_6B_2O_{17}$  systems, we performed parallel experiments on the quinary  $(Zr_3Hf_3)(NbTa)O_{17}$  system. Figure 6 and Fig. 7 show the in situ X-ray intensity map and ex situ isothermal scans, respectively. Diffracted intensity from the 811 reflection emerges  $\sim 940$  °C, and full conversion is being approached (as indicated by precursor peak disappearance)  $\sim 1100$  °C.

The 811 reflection emerges in the in situ X-ray intensity map at lower temperatures than in all but the least refractory  $Zr_6Nb_2O_{17}$  ternary permutation. Additionally, the precursor phase peak intensities fall nearly simultaneously in the same temperature range where  $A_6B_2O_{17}$  peaks grow. The simultaneous and continuous precursor peak intensity reduction suggests that the quinary  $A_6B_2O_{17}$  phase forms outright, as opposed to an alternative sequence where multiple ternary endmembers (which are difficult to resolve due to similar interplanar spacings) form in parallel. This is corroborated by ex situ experiments which display unique behavior of the quinary system with



Figure 5 X-ray patterns for ternary  $A_6B_2O_{17}$  phases reacted ex situ at intermediate temperatures.



respect to phase formation temperature relative to any ternary endmember.

The ex situ experiments show that the quinary  $A_6B_2\mathrm{O}_{17}$  phase forms at lower temperatures than three of the associated ternaries despite including the most refractory cations (Hf and Ta). This is consistent with a stronger thermodynamic driving force. Also, unlike the case for  $\mathrm{Zr}_6\mathrm{Nb}_2\mathrm{O}_{17}$ , quinary  $A_6B_2\mathrm{O}_{17}$  formation is not observed after 24 h. at 850 °C. This suggests that the overall reaction sequence is not initial  $\mathrm{Zr}_6\mathrm{Nb}_2\mathrm{O}_{17}$  formation followed by Hf and Ta cation assimilation into a pre-existing  $A_6B_2\mathrm{O}_{17}$  phase (or simultaneous ternary endmember formation). Collectively, these observations are most consistent with working models where (i) higher configurational entropy available in the quinary system drives

phase formation at lower temperatures, or (ii) a more diverse local chemistry available to a quinary system creates faster mass transport pathways. In either case, the more chemically diverse formulation adopts the  $A_6B_2O_{17}$  phase structure after experiencing a lower thermal budget than most of its isostructural endmembers. These observations are also consistent with the larger solid-solubility limits supported in highentropy oxides.

#### **Conclusions**

In this paper, we use a series of diffraction-based experiments to locate minimum stabilization temperatures for ternary and quinary permutations of



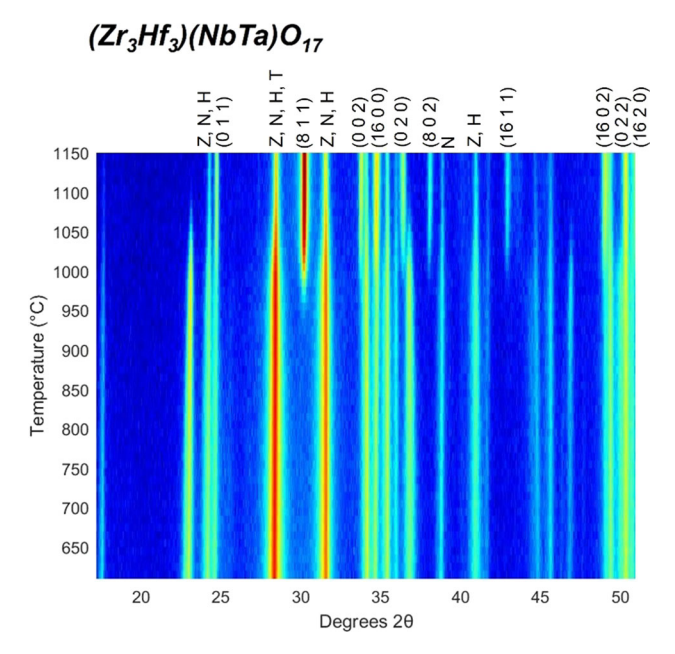


**Figure 6** In situ high-temperature X-ray diffraction for the  $(Zr_3Hf_3)(NbTa)O_{17}$  quinary system.

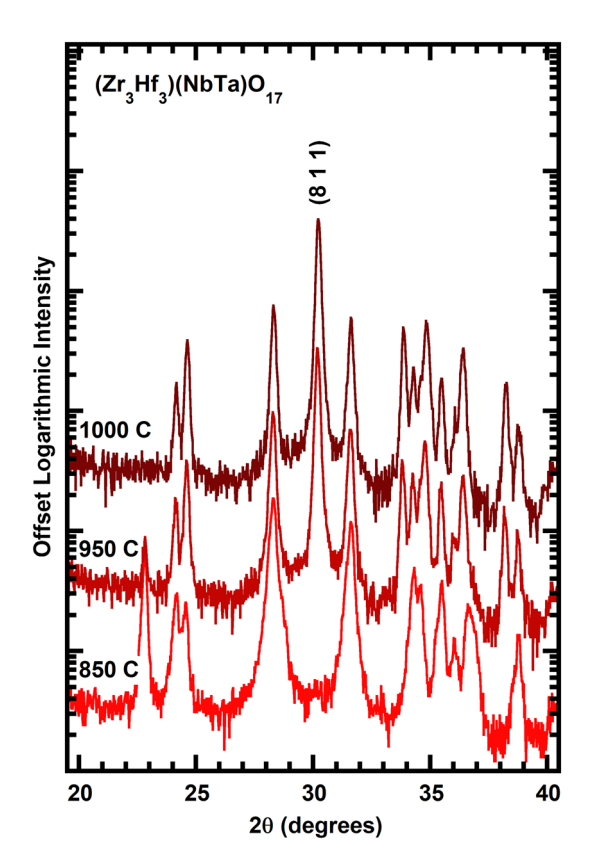


**Figure 7** Ex situ X-ray diffraction studies for the  $(Zr_3Hf_3)(NbTa)O_{17}$  quinary system.

the  $A_6B_2O_{17}$  (A = Zr, Hf; B = Nb, Ta) phase family. We show that these stabilization temperatures are inline with previous literature predictions, suggesting that these phases are substantially to fully disordered with respect to the cation sublattice. While the refractory nature of the binary precursor oxides induces slow reaction kinetics, which in turn makes absolute stabilization temperature identification difficult, we find that our results are generally in agreement with the literature. Furthermore, we observe that the quinary (Zr<sub>3</sub>Hf<sub>3</sub>)(NbTa)O<sub>17</sub> phase experiences a comparatively lower stabilization temperature than most of the ternary endmember  $A_6B_2O_{17}$  permutations. We propose that this effect results from the cation diversity and thus high configurational entropy of the quinary system.

## Acknowledgements

The authors would like to acknowledge Erik Furton of Pennsylvania State University for his assistance with high-temperature X-ray diffraction data processing, as well as Saeed Almishal for his ongoing participation in discussions on the topic of complex oxide thermodynamic behavior. This material is based upon work supported by the National Science Foundation, as part of the Center for Dielectrics and Piezoelectrics under Grant Nos. IIP-1841453 and IIP-1841466. RJS was supported by the National Science Foundation Graduate Research Fellowship Program under Grant No. DGE1255832. Any opinions, findings, and conclusions or recommendations expressed in this material are those of the authors and do not necessarily reflect the views of the National Science Foundation. CS and JPM acknowledge support through the Office of Naval Research Grant W911NF-16-1-0406. NSM and JPM acknowledge support from the U.S. Department of Defense through the National Defense Science and Engineering Graduate Fellowship through the Office of Naval Research, with additional support through the Office of Naval Research (Naval Research contract N00014-21-1-2515).

## Data availability

Data may be made available by contacting the corresponding author, RJS (rjs7012@psu.edu).



#### **Declarations**

**Conflicts of interest** The authors declare that they have no conflicting or competing conflicts of interest.

**Supplementary Information:** The online version contains supplementary material available at https://doi.org/10.1007/s10853-023-08396-5.

#### References

- [1] Rost CM, Sachet E, Borman T, Moballegh A, Dickey EC, Hou D, Jones JL, Curtarolo S, Maria J-P (2015) Entropystabilized oxides. Nat Commun 6:8485
- [2] Gild J, Samiee M, Braun JL, Harrington T, Vega H, Hopkins PE, Vecchio K, Luo J (2018) High-entropy fluorite oxides. J Eur Ceram Soc 38:3578–3584
- [3] Jiang S, Hu T, Gild J, Zhou N, Nie J, Qin M, Harrington T, Vecchio K, Luo J (2018) A new class of high-entropy perovskite oxides. Scripta Mater 142:116–120
- [4] Chen K, Pei X, Tang L, Cheng H, Li Z, Li C, Zhang X, An L (2018) A Five-Component entropy-stabilized fluorite oxide. J Eur Ceram Soc 38:4161–4164
- [5] Sarkar A, Djenadic R, Wang D, Hein C, Kautenburger R, Clemens O, Hahn H (2018) Rare earth and transition metal based entropy stabilised perovskite type oxides. J Eur Ceram Soc 38:2318–2327
- [6] Vayer F, Decorse C, Bérardan D, Dragoe N (2021) New entropy-stabilized oxide with pyrochlore structure: Dy2(Ti0.2Zr0.2Hf0.2Ge0.2Sn0.2)2O7. J Alloys Compd 883:160773
- [7] Spiridigliozzi L, Ferone C, Cioffi R, Accardo G, Frattini D, Dell'Agli G (2020) Entropy-stabilized oxides owning fluorite structure obtained by hydrothermal treatment. Materials 13:558
- [8] Dabrowa J, Stygar M, Mikuła A, Knapik A, Mroczka K, Tejchman W, Danielewski M, Martin M (2018) Synthesis and microstructure of the (Co, Cr, Fe, Mn, Ni) 3 O 4 high entropy oxide characterized by spinel structure. Mater Lett 216:32–36
- [9] Vinnik DA, Trofimov EA, Zhivulin VE, Zaitseva OV, Gudkova SA, Starikov AYu, Zherebtsov DA, Kirsanova AA, Häßner M, Niewa R (2019) High-entropy oxide phases with magnetoplumbite structure. Ceram Int 45:12942–12948
- [10] Tseng K-P, Yang Q, McCormack SJ, Kriven WM (2020) High-entropy, phase-constrained, lanthanide sesquioxide. J Am Ceram Soc 103:569–576

- [11] Chen K, Ma J, Wang H, Li C, An L (2021) Entropy-stabilized oxides with medium configurational entropy. Ceram Int 47:9979–9983
- [12] Jiang B, Bridges CA, Unocic RR, Pitike KC, Cooper VR, Zhang Y, Lin D-Y, Page K (2021) Probing the local site disorder and distortion in pyrochlore high-entropy oxides. J Am Chem Soc 143:4193–4204
- [13] Oses C, Toher C, Curtarolo S (2020) High-entropy ceramics. Nat Rev Mater 5:295–309
- [14] Sarkar A, Breitung B, Hahn H (2020) High entropy oxides: the role of entropy enthalpy and synergy. Scr Mater 187:43–48
- [15] McCormack SJ, Navrotsky A (2021) Thermodynamics of high entropy oxides. Acta Mater 202:1–21
- [16] Spurling RJ, Lass EA, Wang X, Page K (2022) Entropydriven phase transitions in complex ceramic oxides. Phys Rev Mater 6:090301
- [17] Bérardan D, Franger S, Dragoe D, Meena AK, Dragoe N (2016) Colossal dielectric constant in high entropy oxides. Phys Status Solidi RRL 10:328–333
- [18] Chen H, Fu J, Zhang P, Peng H, Abney CW, Jie K, Liu X, Chi M, Dai S (2018) Entropy-stabilized metal oxide solid solutions as CO oxidation catalysts with high-temperature stability. J Mater Chem A 6:11129–11133
- [19] Mao A, Xiang H-Z, Zhang Z-G, Kuramoto K, Zhang H, Jia Y (2020) A new class of spinel high-entropy oxides with controllable magnetic properties. J Magn Magn Mater 497:165884
- [20] Mao A, Xie H-X, Xiang H-Z, Zhang Z-G, Zhang H, Ran S (2020) A novel six-component spinel-structure high-entropy oxide with ferrimagnetic property. J Magn Magn Mater 503:166594
- [21] Jothi PR, Liyanage W, Jiang B, Paladugu S, Olds D, Gilbert D, Page K (2022) Persistent structure and frustrated magnetism in high entropy rare-earth zirconates. Small 18:2101323
- [22] McCormack SJ, Kriven WM (2019) Crystal structure solution for the A6B2O17 (A = Zr, Hf; B = Nb, Ta) super-structure. Acta Cryst 75:227–234
- [23] Voskanyan AA, Lilova K, McCormack SJ, Kriven WM, Navrotsky A (2021) A new class of entropy stabilized oxides: commensurately modulated A6B2O17 (A = Zr, Hf; B = Nb, Ta) structures. Scripta Mater 204:114139
- [24] Galy J, Roth RS (1973) The crystal structure of Nb2Zr6O17.
  J Solid State Chem 7:277–285
- [25] Luo P, Wu X, Xiao W, Zhang F, Wang Y, Huang D, Du Y (2022) Phase equilibria in the ZrO<sub>2</sub>–Ta<sub>2</sub>O<sub>5</sub>–Nb<sub>2</sub>O<sub>5</sub> system: experimental studies and thermodynamic modeling. J Am Ceram Soc 105:668–686



[26] Tan ZY, Xie ZH, Wu X, Guo JW, Zhu W (2023) Spark plasma sintering of A6B2O17 (A = Hf, Zr; B = Ta, Nb) high entropy ceramics. Mater Lett 330:133381

**Publisher's Note** Springer Nature remains neutral with regard to jurisdictional claims in published maps and institutional affiliations.

Springer Nature or its licensor (e.g. a society or other partner) holds exclusive rights to this article under a publishing agreement with the author(s) or other rightsholder(s); author self-archiving of the accepted manuscript version of this article is solely governed by the terms of such publishing agreement and applicable law.

